LONDON, METEOROLOGICAL OFFICE.
Met.O.15 Internal Report No. 72.

The accuracy of cross-chain LORAN-C wind measurement in the United Kingdom area.

08210487 FH5B

METEOROLOGICAL OFFICE
London Road, Bracknell, Berks.

MET.O.15 INTERNAL REPORT

No 72

The Accuracy of Cross-Chain LORAN-C Wind Measurement in the United Kingdom Area

by

S.A. Clough, M Greengrass and P.G.W. Healey

March 1987

Cloud Physics Branch (Met.O.15)

The Accuracy of Cross-Chain LORAN-C Wind Measurement in the United Kingdom Area.

By S.A.Clough, M.Greengrass and P.G.W.Healey.

March 1987.

Abstract

Details are given of a new method for calculating wind velocities using the Loran-C hyperbolic navigation system so as to utilise all the available transmitters. Trial results involving radar tracking of sondes are presented which demonstrate that RMS vector accuracies better than +/- 2 knots can be achieved in 1-minute winds.

1. Introduction

Wind measurement in the Meteorological Office aircraft dropsonde system is carried out by tracking the difference in times of arrival of Loran-C signal pulses. In the current system, signals received from three Loran transmitters within a chain are used to determine position, providing the basis for calculating windspeeds. High precision computation gives a time sequence of positions, the differential of which is the velocity.

The method, however, is limited in that it does not generalise to the situation where more than three transmitters are available. Since the expansion of Loran-C in recent years, output from several transmitters may be usable at a location, particularly with cross chain operation which is now possible with the new dropsonde system. In common with the work of Lally & Morel (1985), the approach discussed below incorporates all of the available data, using a weighted least squares solution to remove the redundancy which results when four or more transmitters are involved. As well as appropriate geometrical factors, estimated errors are specified for each transmitter, and these determine the weighting for each contribution to the calculated velocity.

There are a number of important advantages of this new method of wind computation :

(i) The accuracy is less critically dependent upon the appreciable change in geometrical factors with location, and the variability of signals from individual transmitters. Thus, high quality wind measurement is not subject to the severe geographical constraints previously noted in three-transmitter operation (Ryder, 1975).

(ii) Rather than recalculating the position at each time step, the new method updates a given starting position by integrating the velocities as they are found. This retains accuracy (as demonstrated below) whilst reducing the amount of high precision computation required. For a given location and error weights, winds are determined from time differences by a single matrix multiplication, so that real time implementation is also economical and straightforward.

(iii) A convenient means of estimating the accuracy of results arises during the processing.

(iv) Because there is data redundancy in the system, the veracity of

features of interest (eg rapid changes or oscillations) can be checked, and distinguished from spurious effects.

We shall first summarise the theory involved, and go on to discuss the factors affecting Loran transmission and use. A method is suggested for assigning a weight to signals from each transmitter, and this is used to compare Loran wind measurements with results from tracking of sondes by radar. Finally, estimates of the expected accuracy of wind measurement are given for various locations. On the basis of laboratory monitoring, a typical value of +/- 0.39 knots is estimated for a receiver at Bracknell.

2. Theory

The theory used here is parallel to the principles used in Omega wind computation, as discussed by Franklin & Julian (1985). The matrix approach to weighted least squares calculations is a standard technique, but the details are given here for completeness. (See also Gold 1974, upon which this account is based.)

Let $\underline{u}$ denote the computed value of the actual velocity $\underline{u_A}$ based on a set of n measurements $\underline{z}$. For this problem, n is the number of independent Loran time differences available, ie one less than the number of transmitters used. We assume that $\underline{z}$ can be expressed as a vector sum of the form :

$$\underline{z} = \underline{F}\underline{u_A} + \underline{s} \qquad \ldots (1)$$

where $\underline{F}$ is an n x 2 matrix containing geometrical factors,
and $\underline{s}$ is a random measurement error.

To choose the estimate $\underline{u}$, we shall minimise the sum of the squares of the deviations $\underline{z} - \underline{F}\underline{u}$,

ie minimise :

$$J = (\underline{z} - \underline{F}\underline{u})^T (\underline{z} - \underline{F}\underline{u}) \qquad \ldots (2)$$

with respect to $\underline{u}$.

The derivation is given in Appendix A, and the best estimate of $\underline{u_A}$ is found to be :

$$\underline{u} = (\underline{F}^T \underline{F})^{-1} \underline{F}^T \underline{z} \qquad \ldots (3)$$

To incorporate weighting, we minimise :

$$J = (\underline{z} - \underline{F}\underline{u})^T \underline{E}^{-1} (\underline{z} - \underline{F}\underline{u}) \qquad \ldots (4)$$

where $\underline{E}^{-1}$ is an n x n weighting matrix.

The form of the weighting matrix is determined by taking each weight to be inversely proportional to the measurement error. $\underline{E}$ then corresponds to the covariance matrix of $\underline{s}$.

Following the procedure adopted by Passi (1973), the elements of $\underline{E}$ are given by the variances of the rates of change of measured time difference :

$$e_{ij} = s_1^2 + s_0^2 \quad \text{for } i = j$$
$$= s_0^2 \quad \text{otherwise.} \qquad \ldots (5)$$

Where s_0 refers to the contribution from the chosen master transmitter. The choice of values for s_1 is discussed below.

When the covariance matrix $\underline{E}$ is incorporated, the result (3) above becomes :

$$\underline{u} = (\underline{F}^T \underline{E}^{-1} \underline{F})^{-1} \underline{F}^T \underline{E}^{-1} \underline{z} \qquad \ldots (6)$$

The most complex process in calculating the expression pre-multiplying $\underline{z}$ in Equation (6) is inverting $\underline{E}$, which is a square matrix of order n. (Since $\underline{E}$ is symmetric and positive definite, this is readily done by Cholesky decomposition, which for n = 5 only takes about 1 second on a microprocessor. For real time application this inversion only needs to be carried out ocassionally when large ghanges in weights occur)

As was also pointed out by Passi, the estimated wind error dU is given by :

$$dU^2 = \text{Trace} ((\underline{F}^T \underline{E}^{-1} \underline{F})^{-1}) \qquad \ldots (7)$$

The proof of this result is given in Appendix B. The expression inside the brackets arises naturally when Equation (6) is applied, giving a convenient error estimate.

To summarise, given n + 1 transmitters, we can form n independent time differences. The rates of change of these at each time step comprise the vector $\underline{z}$. Equation (6) states that we will obtain an optimum estimate for the velocity vector $\underline{u}$ from the measurements $\underline{z}$, using an n x 2 matrix of geometrical factors $\underline{F}$ (described in Appendix C), and an n x n covariance matrix $\underline{E}$.

3. Loran-C Transmission

The main difficulty encountered in applying the above method lies in the choice of s_i values to describe the likely error in time of arrival of signals associated with each Loran transmitter. Whilst there is no problem for a location where measurements can be made using static monitoring, where this is not possible some method has to be found of relating s_i at the current position to a value for a different position where monitoring was possible. The procedure adopted by Ryder (1975) for a priori estimation was to develop an empirical formula relating s_i to the transmitter power and its range. A simple inverse square relationship was assumed, which in practice is of limited applicability, because the overall behaviour of the system is rather more complex, and a variety of factors come into play. To appreciate these, a brief discussion of Loran-C transmissions is required. (For a more detailed treatment see Frank, 1983.)

The signals transmitted take the form of groups of eight pulses. Each pulse has an envelope lasting about 200 microseconds, which contains radio frequency oscillations of period 10 microseconds (Fig.1). The low frequency used (90-110kHz) causes the signal arriving at a distant receiver to have two distinct parts - a ground wave and a sky wave. The ground wave is the intended carrier of Loran, which travels along the Earth's surface. The sky wave is the result of reflections from the ionosphere, and includes components which have suffered one or more such reflections. The sky wave path is always longer than that of the ground wave, so that the ground wave is the first to arrive.

Fig.2 shows the dependence of the sky wave delay upon distance, and also upon the height of the ionospheric E layer where reflections occur. Clearly this height will affect the path length, and it has marked diurnal variations arising from changes in electron density. (See Terman, 1943, p.710ff.) During the day, the E layer height is around 70km, but at night it rises to 90km. Dusk/dawn variations are the strongest, and can result in loss of tracking, as has been observed at times during 24hr monitoring of signals at Bracknell from the Sandur transmitter in Iceland (2000km). Looking at the largest ranges on Fig.2, and using the daytime curve, the minimum sky wave delay in regions of viable operation is seen to be about 50 microseconds.

Predicting the intensities of the ground and sky waves is not easy. In the ground wave case, the main reason for this is that the strength of the propagating signal is a function of the path over the Earth. The conductivity of land is low compared to that of sea, and thus signals from transmitters with considerable land paths are poorer than signals over sea tracks. Weather conditions will also affect the intensity of a Loran signal, and this can give appreciable day to day variations. The sort of distance dependence observed for Loran signal strength under various circumstances is shown in Fig.3.

Under ideal conditions, a Loran-C receiver tracks the third zero crossing inside each ground wave pulse. As the sky wave pulse delay

is greater than 30 microseconds, there should be no interference between the two for a receiver of large bandwidth. However, this means that the ground wave pulse amplitude has not risen to its full value when the measurement is made, so that signal to noise ratio (SNR) is reduced. In noisy conditions it is often necessary to track further into the the pulse envelope and the sky wave may then interfere, particularly if a narrow bandwidth is being used to increase the SNR. Because of interference between the sky and ground wave components, an increased variability of phase may be expected as distance increases.

The effect of the mixing of skywave with groundwave is apparent in Fig.4. These graphs are the result of monitoring 3 Loran transmitters for most of a day in late spring using a static receiver at Eskmeals, Cumbria, and each shows the time of arrival (TOA) of the pulse from one of the transmitters as a function of time. The linearly increasing trend of TOA is purely the result of oscillator drift and is unimportant. Fig.4(a) shows that for the nearest transmitter Sylt in North Germany (750km) the phase is virtually constant, and the signal is dominated by the ground wave. Fig.4(b) for Ejde in the Faeroes (900km) has some sky wave components mixed in, and significant deviations from a straight line are evident. Fig.4(c) is for the most distant transmitter Sandur in Iceland (1600km). Here, the coherence of the signal is sometimes lost completely because of the large and varying amount of skywave. Only very rapid phase changes will give a significant bias contribution to the error of wind measurements, so this is unlikely to be a problem in most cases, but the poor signal to noise behaviour near dusk and dawn can cause serious difficulties where sky wave dominates. Ryder's method of estimating a priori sigma values on the basis of an estimate of received power at a given location cannot cope with such variations at all. In view of the complexity of the problem, an alternative method was adopted here, which will be discussed next.

4. Results

This section first describes the measurements made to assign appropriate weightings to Loran signals of different qualities. The results of a trial of the new dropsonde system analysed by the above method are presented, and allow assessment of the accuracy estimates given by equation (7). Finally, initial error estimates are made for different locations. Note that all velocity figures quoted are for 1-minute wind values.

(a) Relationship of Variance to SNR

The first step was to find the relationship between variance and the SNRs measured using static monitoring. For the actual position where measurements are to be made, the SNR can be estimated a priori to obtain initial variance estimates, and the prevailing SNR values can then be used to give more accurate values of variance in real time.

Monitoring of signals was carried out using both the existing Beukers LOCATE system and the new system during its development. For a static receiver at Bracknell, the three transmitters in the SL3 (Norwegian Sea) Loran-C chain were monitored over several days. The new system also allowed monitoring of the two extra transmitters in the French Loran chain. Averaging in blocks of half-hour duration, figures for mean SNR and standard deviation of rate of change of time of arrival were calculated. Each such block gives one point on Figs. 5 and 6.

For a static receiver, TOA varies linearly with time as a result of oscillator drift. Noise (which may be true noise, or fluctuations caused by interference between ground and sky waves) results in small fluctuations around this straight line. Thus we look at the standard deviation of the gradient of TOA, because this will be related to the SNR. This is the reason underlying the relationships of Figs. 5 and 6. A straight line fit was used for Fig.5, while an exponential was found to be better for Fig.6.

Note that the SNR measurements are specific to the equipment used. This arises because the SNR is determined by statistical theory (see Ryder, 1976) from a signal sample taken in the tracking process, and the ability to distinguish SNR accurately depends upon the timing of the sample. For the Beukers LOCATE equipment the sample is made 1/4 of a cycle after the zero crossing, whereas the new system uses 1/10 of a cycle, giving better discrimination over the SNR range. Another difference is that the new system uses 15-second smoothed SNR values to determine the tracking coefficients used, and this makes it more responsive to variations in signal quality. As is apparent from comparing Figs. 5 and 6, the nominal SNR values are completely different for the two systems. The new system tracks poor signals somewhat better than the LOCATE system, though the trial results (see below) indicate occasional erratic and unreliable behaviour at the lowest SNRs recorded.

(b) Comparison with Radar Data

In collaboration with the Met O 1b trials team, a comparison with radar tracked sondes was carried out. Balloon-borne Vaisala RS80 Loran sondes were used for the exercise, launched from Beaufort Park and tracked by the Beaufort Park Cossor radar. The Loran tracking was performed by the Met O 15 laboratory in Bracknell using omnidirectional and Yagi aerials on the roof of the Dynes wing. Some practical difficulties were experienced with both the radar and dropsonde systems. The radar had a hardware fault which reduced the reliability of the first sounding somewhat, while reception of signals in Met O 15 was at times adversely affected by shadowing from surrounding buildings, and lock-on to the signal was not possible until after launch. Also, the Met. Office building may have a fairly high background noise level due to traffic ignition and miscellaneous electrical sources, particularly computer equipment. Nonetheless, six usable soundings of up to one and a half hours were obtained under a range of conditions.

Figs. 7 - 12 show superimposed radar and Loran 1-minute wind soundings for the six flights and their vector differences. Note that the first part of the radar data for Flight 3 is missing as a result of losing track of the sonde, and the end of the Loran data for Flight 6 was accidentally corrupted on the tape. The Loran data for Flight 4 had two obviously erroneous regions near the beginning, and these are omitted from the plots. (This flight is discussed further in Section (c) below.) The radar measurement uncertainty increased after the balloons carrying the sondes burst, so the graphs terminate at or before burst time as determined from the radar height measurements. The quality of retransmitted Loran signals was found to improve after burst, as is apparent from Fig.14, but the reason for this is unclear.

The magnitude of the vector difference between the radar and Loran velocities was calculated every 15 seconds. Table 1 shows the RMS of these magnitudes over 15-minute periods, and provides upper bound estimates on the accuracy of Loran tracking. (Particular care was needed in the comparisons to ensure that there was no misalignment in time.) The majority of values are less than 2 knots, representing very good agreement.

Tables 2 and 3 give average differences in the U and V components respectively for the same data as Table 1. The actual values for Flight 5 are plotted in Fig.13 as an example. There is no evidence of any significant bias in either of the components. Integrating the figures in Table 1 over time gives an indication of the size of any cumulative positional error introduced by the way position is updated using the calculated velocities during Loran processing. (It is assumed that any positional error in the radar is not cumulative.) The error found in this way after one hour is up to about 4km (although bad Loran data such as in Flight 4 could cause problems). This distance constitutes a negligible change in the Loran geometry, and no appreciable error in wind measurements will result from this source.

One feature which is apparent from Figs. 7 - 12 is that the response of the two systems seems to differ slightly at the boundaries between

shear layers. For example, at 31 minutes into Flight 2 (Fig.8(a)) there is a peak in velocity at which the radar has given a slightly higher value than the Loran system. Such a difference could arise for a number of reasons. The possibility that oversmoothing of the Loran data might be responsible was investigated, but experiments using 15 seconds instead of the standard 30 seconds as the time constant in the 6-pole Bessel filter applied to the 1-second TOAs did not support this hypothesis. The method of computation of the 1-minute winds was the same for both radar and Loran (using the vector joining the positions at the beginning and end of the period) so this would not account for the difference. A likely explanation is that small residual timing errors remain between the two sets of velocities, and this would account for larger errors at points of strong shear. (An example of this occurs 27 minutes into Flight 5 : the sharp peak in radar velocities is also found to be present in the full 1-second Loran data, but at a slightly earlier time.) Alternatively, the damping applied to the respective tracking systems may well differ at this precision. Two methods might be used to study or improve on this performance : comparison with a precision military tracking radar could provide the shorter period performance necessary, while the sensitivity to Loran tracking parameters could be optimised empirically by using several Loran tracking modules in parallel.

(c) Verification of Estimated Wind Measurement Errors

The ability to estimate wind errors reliably from the Loran signals provides useful operational guidance both in the choice of which stations to use and in real time velocity calculations. Table 4 gives estimated wind errors obtained from equation (7) and the graph in Fig.6, averaged so as to allow direct comparison with Table 1. Since the Table 1 figures should include a comparable contribution from the errors of radar velocity measurement, it appears that the estimates of Table 4 provide good guidance to Loran wind errors.

While the choice of sigma by means of SNR is generally a useful method, it cannot cope during periods when the Loran data for a particular transmitter is erroneous at low SNR. A transmitter cannot always be assigned a low enough weight to prevent its affecting the calculated velocity, and in such cases it is better to omit that station completely. This was done with the Icelandic Sandur transmitter for Flights 3 - 6, as its signals are frequently of marginal amplitude in South-East England, especially during Winter.

Graphs of SNR against time for Flight 4 are given in Fig.14 for each transmitter. The signals from Ejde (Fig.14(c)) at the beginning and end of this flight were particularly poor for short periods. The transmitter could have been omitted (as had already been done with Sandur) but was left in the calculations here as an illustration. This meant that there were two intervals when no meaningful winds could be obtained, corresponding to the gaps in the traces on Fig.10. The error estimates in Table 4 indicate larger values at the beginning and end of the flight, with a spell of good accuracy in the middle. This is in line with the observed RMS figures in Table 1, and is also apparent in Fig.10(a). The curves are nearly coincident in the region around 45

minutes into the flight whereas the agreement is less good at other times.

(d) Wind Measurement Accuracy Estimates for Different Positions

As is apparent from the above discussions and Figs. 5, 6 and 14, the SNR at the monitoring location for a given transmitter varies considerably with time of day and atmospheric conditions. The problem becomes even more difficult when the SNR value for an arbitrary location via sonde retransmission is required. It was not found possible to obtain a satisfactory empirical relationship for predicting this, so that to determine the SNR (and hence the error of wind measurements) in advance, one can only rely on informed guesswork based on previous experience. Any accuracy estimate will have to be modified in the light of the SNR values prevailing when the winds are measured.

To obtain rough estimates of the expected accuracy of computed winds, the range of each transmitter was calculated for various positions. An SNR for a given transmitter was adopted by comparing its range with those of the transmitters at Bracknell, where average SNR values are available (at least in the laboratory). This procedure is set out in Tables 5 and 6, and the results are shown on Fig.15 in relation to the experimental areas to be used in the forthcoming Mesoscale Frontal Dynamics Project (Autumn 1987).

Under favourable conditions, this method predicts that accuracies will be better than 1 Knot, but it must be borne in mind that the prevailing SNR values could differ appreciably from those estimated. For example, the estimated value for dU at Bracknell in Fig.15 (0.39 knots) is rather lower than the figures in Table 4. This is because the mean SNRs in the laboratory monitoring were larger than those measured during the field trials, and hence the station variances from Fig.6 were correspondingly less. When the equipment is used on board the Met. Office Hercules C-130 research aircraft the SNRs are likely to be different again, so that quantitative accuracy estimates will only be obtainable at the time of measurement.

5. Conclusions

(i) A least squares solution has been developed to utilise all available Loran-C data for wind measurement.

(ii) Using an empirical approach, a system of assigning relative weights to the Loran transmitters was found. This involves relating the error to the signal to noise ratio (SNR) prevailing for each transmitter.

(iii) Calculated velocities were compared with independent radar measurements, and agreement to better than 2 knots was achieved in most cases. This is thought to be close to the limit attainable by the Cossor radar itself, and to get a more stringent check on the accuracy of Loran winds (particularly over half-minute periods and hence 300m resolution for the dropsonde) further comparison with a precision military tracking radar would be necessary.

(iv) A method of estimating the velocity error from Loran measurements was found to produce realistic figures in the radar comparisons provided that SNR values are known for each transmitter, and are above a threshold level. This threshold level, however, is extremely low and corresponds to signals which are barely operable. The most likely problems at low SNR under typical operating conditions would be caused by dusk/dawn transitions.

(v) Estimates of the expected accuracy of wind measurements at selected positions in the South West approaches were calculated by estimating the SNR from measurements made at Bracknell. These were found to be better than 1 knot, though verification under typical observing conditions should be attempted.

References

Frank R.L., "Current developments in Loran-C.", Proc. IEEE, 71, No.10, 1127-1139, (1983).

Franklin J.L. and Julian P.R., "An investigation of Omega windfinding accuracy.", J. Atmos. Oceanic Tech., 2, 212-231, (1985).

Gold A. (Ed.), "Applied optimal estimation.", Analytic Sciences Corp., 23-24 and 102-103, (1974).

Lally V.E. and Morel C., "Wind measurements using all available Loran stations.", Wild Goose Assoc., Proc. 14th An. Tech. Symp., 84-96, (1985).

Lee A.C.L., Unpublished report, Met O 15, (1985).

Passi R.M., "Wind determination using Omega signals.", J. Appl. Met., 13, 934-939, (1974).

Ryder P., "The accuracy of wind finding using the Loran-C navigation system.", Unpublished report, Met O 15, (1975).

Ryder P., "Description and optimisation of the LOCATE tracking algorithm for use with Loran-C.", Unpublished, Met O 15 Int. Report No.16, (1976).

Terman F.E., "Radio engineers' handbook.", McGraw Hill, (1943).

Appendix A - Least Squares Estimates

The equation describing the system is :

$$\underline{z} = \underline{F}\underline{u}_{\text{actual}} + \underline{s} \qquad \ldots \text{(A1)}$$

Where $\underline{z}$ is an $n \times 1$ vector (measured)
$\underline{F}$ is an $n \times 2$ matrix (known)
$\underline{u}_{\text{actual}}$ is a 2×1 vector (the actual wind velocity)
and $\underline{s}$ is an $n \times 1$ vector (the random error of measurement).

To choose the optimum value of $\underline{u}$ such that $\underline{u}$ is the best estimate of $\underline{u}_{\text{actual}}$, we minimise the sum of squares of deviations $(\underline{z} - \underline{F}\underline{u})$.

$$J = (\underline{z} - \underline{F}\underline{u})^T (\underline{z} - \underline{F}\underline{u}) \qquad \ldots \text{(A2)}$$

Minimise J with respect to $\underline{u}$.

$$\frac{dJ}{d\underline{u}} = 0 \qquad \ldots \text{(A3)}$$

ie $$\frac{d}{d\underline{u}} \left((\underline{z} - \underline{F}\underline{u})^T (\underline{z} - \underline{F}\underline{u}) \right) = 0$$

$$\frac{d}{d\underline{u}} \left(\underline{z}^T \underline{z} - \underline{z}^T \underline{F}\underline{u} - (\underline{F}\underline{u})^T \underline{z} + (\underline{F}\underline{u})^T \underline{F}\underline{u} \right) = 0$$

$$0 - \frac{d}{d\underline{u}} \left((\underline{F}^T \underline{z})^T \underline{u} \right) - \frac{d}{d\underline{u}} (\underline{u}^T \underline{F}^T \underline{z}) + \frac{d}{d\underline{u}} (\underline{u}^T \underline{F}^T \underline{F}\underline{u}) = 0$$

Using the identities :

$$\frac{d}{d\underline{x}} (\underline{y}^T \underline{x}) = \underline{y} \qquad \text{and} \qquad \frac{d}{d\underline{x}} (\underline{x}^T \underline{y}) = \underline{y} \qquad \ldots \text{(A4)}$$

along with the product rule, allows us to simplify this to :

$$-2 \underline{F}^T \underline{z} + 2 \underline{F}^T \underline{F}\underline{u} = 0$$

$$\Rightarrow \quad \underline{u} = (\underline{F}^T \underline{F})^{-1} \underline{F}^T \underline{z} \qquad \ldots \text{(A5)}$$

This gives the least squares estimate of the actual value $\underline{u}_{\text{actual}}$.

Appendix B - Velocity Error Estimation

Assume to begin with that no error is involved in the measurements.

$$\underline{z_A} = \underline{F}\,\underline{u_A} \qquad \ldots \text{(B1)}$$

If we now consider small error fluctuations around $\underline{z_A}$ and $\underline{u_A}$:

$$\underline{dz} = \underline{F}\,\underline{du} \qquad \ldots \text{(B2)}$$

Then the covariance matrix will be given by :

$$\underline{E} = (\underline{dz}\ \underline{dz}^T) = \underline{F}\underline{du}\ (\underline{F}\underline{du})^T$$

$$= \underline{F}\ \underline{du}\ \underline{du}^T\ \underline{F}^T \qquad \ldots \text{(B3)}$$

Take the case where $n = 2$, so that $\underline{F}$ is a square matrix which we assume is non-singular.

$$\underline{F}^{-1}\ \underline{E} = \underline{du}\ \underline{du}^T\ \underline{F}^T$$

$$\Rightarrow \quad \underline{du}\ \underline{du}^T = \underline{F}^{-1}\ \underline{E}\ (\underline{F}^T)^{-1}$$

$$= (\underline{F}^T\ \underline{E}^{-1}\ \underline{F})^{-1} \qquad \ldots \text{(B4)}$$

Considering the left hand side, and writing $\underline{du}$ in component form :

$$\underline{du}\ \underline{du}^T = \begin{pmatrix} du \\ dv \end{pmatrix} \ (\ du\ dv\ ) = \begin{pmatrix} du^2 & dudv \\ dudv & dv^2 \end{pmatrix}$$

So,

$$\text{Trace}\ (\underline{du}\ \underline{du}^T) = du^2 + dv^2 = (\ \text{Wind error}\ )^2 \qquad \ldots \text{(B5)}$$

The wind error may thus be conveniently calculated using :

$$(\ \text{Wind error}\ )^2 = \text{Trace}\ (\ (\underline{F}^T\ \underline{E}^{-1}\ \underline{F})^{-1}\ ) \qquad \ldots \text{(B6)}$$

Appendix C - Calculation of Matrix F

The matrix $\underline{F}$ relates the actual velocity to the measurements of rate of change of time difference perpendicular to each of the lines of position (LOP's).

ie If $\underline{z_A}$ represents an ideal set of measurements with no error, then :

$$\underline{z_A} = \underline{F}\,\underline{u_A} \qquad \ldots (C1)$$

Converting a rate of change of time difference into a velocity perpendicular to the LOP involves multiplying by a scale factor :

$$\Gamma_i = \frac{c}{2 \sin (\phi_i / 2)} \qquad \ldots (C2)$$

where c is the velocity of propagation of the Loran signals, and ϕ_i is the difference between the bearings to the two transmitters which are associated with that LOP.

If the LOP direction is designated Ψ_i , and the two components of $\underline{u_A}$ are u_A and v_A , then resolving perpendicular to the LOP (Fig.16) :

$$- u_A \cos \Psi_i + v_A \sin \Psi_i = \Gamma_i z_{Ai} \qquad \ldots (C3)$$

So the $n \times 2$ matrix $\underline{F}$ will contain n rows of the form :

$$- \cos \Psi_i / \Gamma_i \quad , \quad \sin \Psi_i / \Gamma_i \qquad \ldots (C4)$$

Table 1 - RMS magnitude of vector velocity difference between radar and Loran 1-minute winds over 15-minute periods.

Sonde Flight Number and Date	0-15	15-30	30-45	45-60	60-75	minutes
1. 3/11/86	0.98	1.42	2.04	2.42	2.61	knots
2. 5/11/86	1.18	1.33	-	-	-	
3. 10/12/86-A	-	1.48	1.22	1.34	2.03	
4. 10/12/86-B	2.42	2.47	1.45	1.58	2.80	
5. 12/12/86-A	0.78	1.30	1.14	1.64	-	
6. 12/12/86-B	1.24	2.04	-	-	-	

Table 2 - Average difference in u-component (radar - Loran) for 1-minute winds over 15-minute periods.

Sonde Flight Number and Date	0-15	15-30	30-45	45-60	60-75	minutes
1. 3/11/86	0.28	0.60	0.35	-0.28	-0.60	knots
2. 5/11/86	0.14	-0.12	-	-	-	
3. 10/12/86-A	-	0.86	0.08	0.23	0.30	
4. 10/12/86-B	0.84	1.67	0.83	0.62	1.56	
5. 12/12/86-A	0.27	0.43	0.00	0.49	-	
6. 12/12/86-B	0.37	1.23	-	-	-	

Table 3 - Average difference in v-component (radar - Loran) for 1-minute winds over 15-minute periods.

Sonde Flight Number and Date	0-15	15-30	30-45	45-60	60-75	minutes
1. 3/11/86	-0.17	-0.24	-0.18	0.14	0.02	knots
2. 5/11/86	0.14	0.00	-	-	-	
3. 10/12/86-A	-	-0.55	-0.08	0.17	0.32	
4. 10/12/86-B	-0.62	-0.94	-0.16	-0.18	-0.63	
5. 12/12/86-A	-0.03	-0.20	0.28	0.04	-	
6. 12/12/86-B	0.07	-0.58	-	-	-	

Table 4 - Estimated RMS error of Loran wind measurement (dU) averaged for 15-minute periods.

Sonde Flight Number and Date	0-15	15-30	30-45	45-60	60-75	minutes
1. 3/11/86	0.51	0.60	0.80	0.87	0.95	knots
2. 5/11/86	0.56	0.58	0.64	0.82	1.01	
3. 10/12/86-A	0.56	0.45	0.76	0.68	0.64	
4. 10/12/86-B	1.09	0.91	0.37	0.54	1.30	
5. 12/12/86-A	0.43	0.52	0.60	0.64	0.80	
6. 12/12/86-B	0.49	0.49	0.39	0.35	0.43	

Table 5 - Average SNR values measured at Bracknell.

Identifier as used in Table 6	Transmitter	Distance from Bracknell /km	Average SNR /dB
A	Sylt	700	6
B	Sandur	2000	-3
C	Ejde	1300	2
D	Lessay	250	8
E	Soustons	850	1

Table 6 - Ranges of Loran transmitters at selected positions with nearest equivalent from Table 5 above. This allows the estimated RMS error of Loran wind measurement (dU) to be calculated for each position.

Transmitter	50 N, 6 W	46 N, 6 W	46 N, 10 W	48 N, 12 W	
Sylt	1100 C	1400 C	1600 C	1600 C	km
Sandur	1950 B	2350 B	2250 B	2000 B	
Ejde	1350 C	1800 B	1800 B	1600 C	
Lessay	350 D	500 A	725 A	800 E	
Soustons	800 E	450 D	725 A	950 E	
dU	0.54	0.70	0.80	0.93	knots

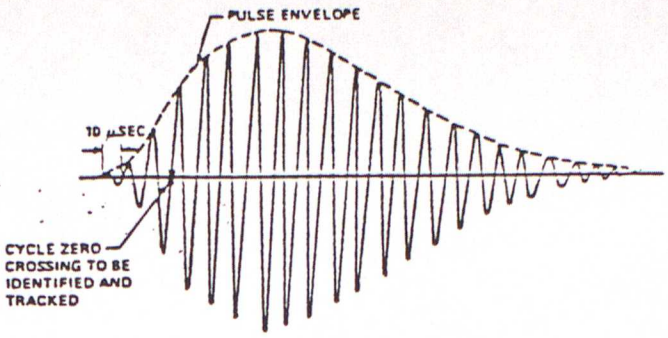

Fig. 1 Loran-C pulse detail.

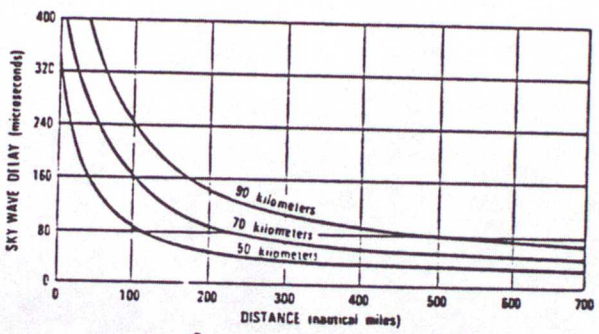

Fig. 2 100-kHz sky-wave delay.

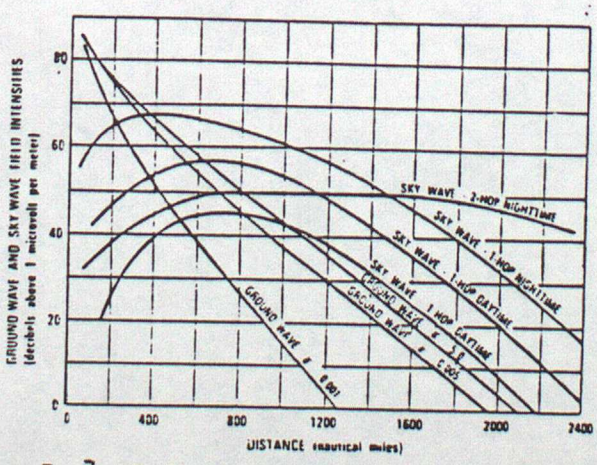

Fig 3 100-kHz signal strengths. 100-kW radiated power.

(Reproduced from Frank, 1983.)

Fig.4 - SL3 chain Loran-C signals received at Eskmeals.

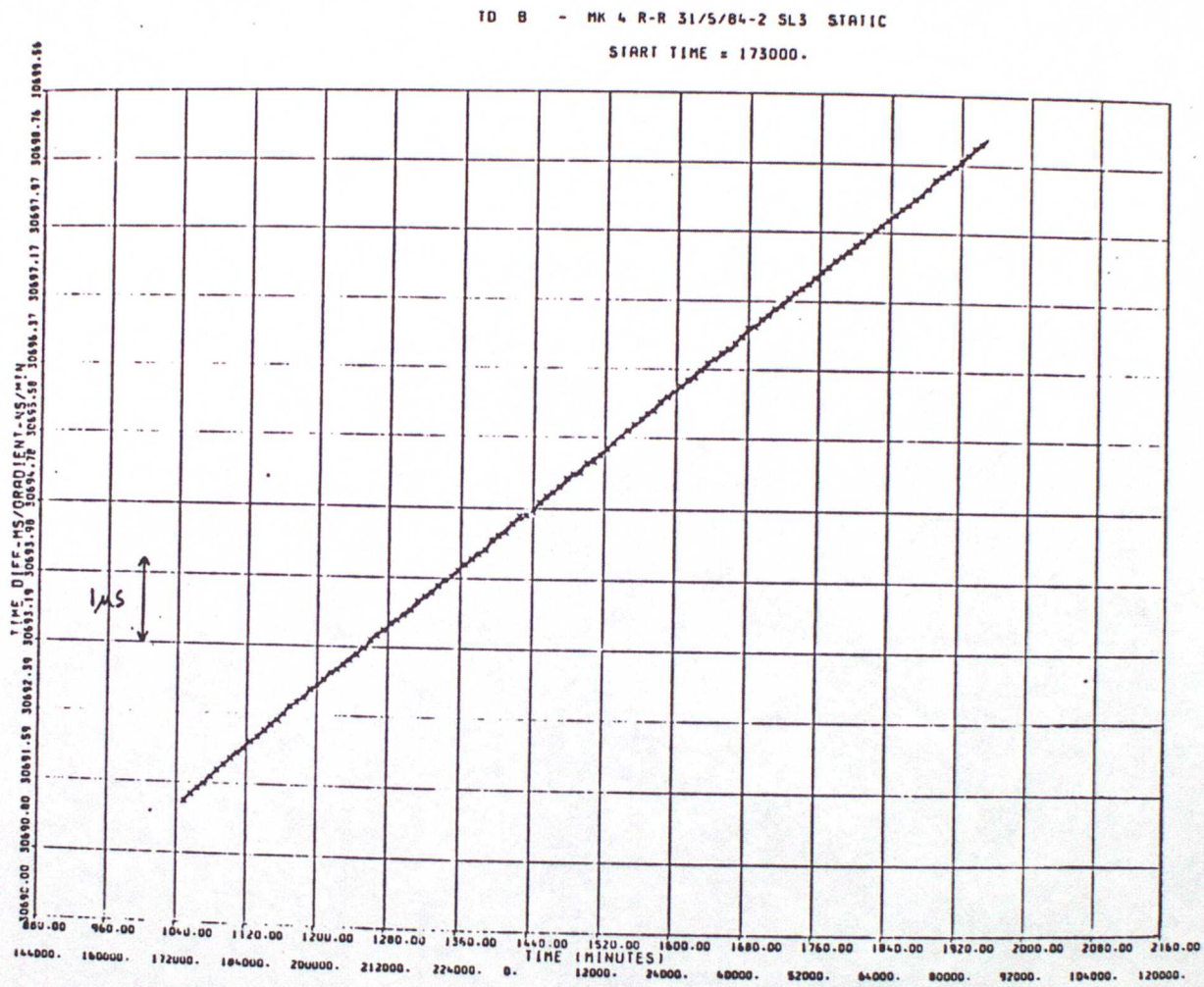

4(a) Sylt (range 750km).

4(b) Ejde (range 900km).

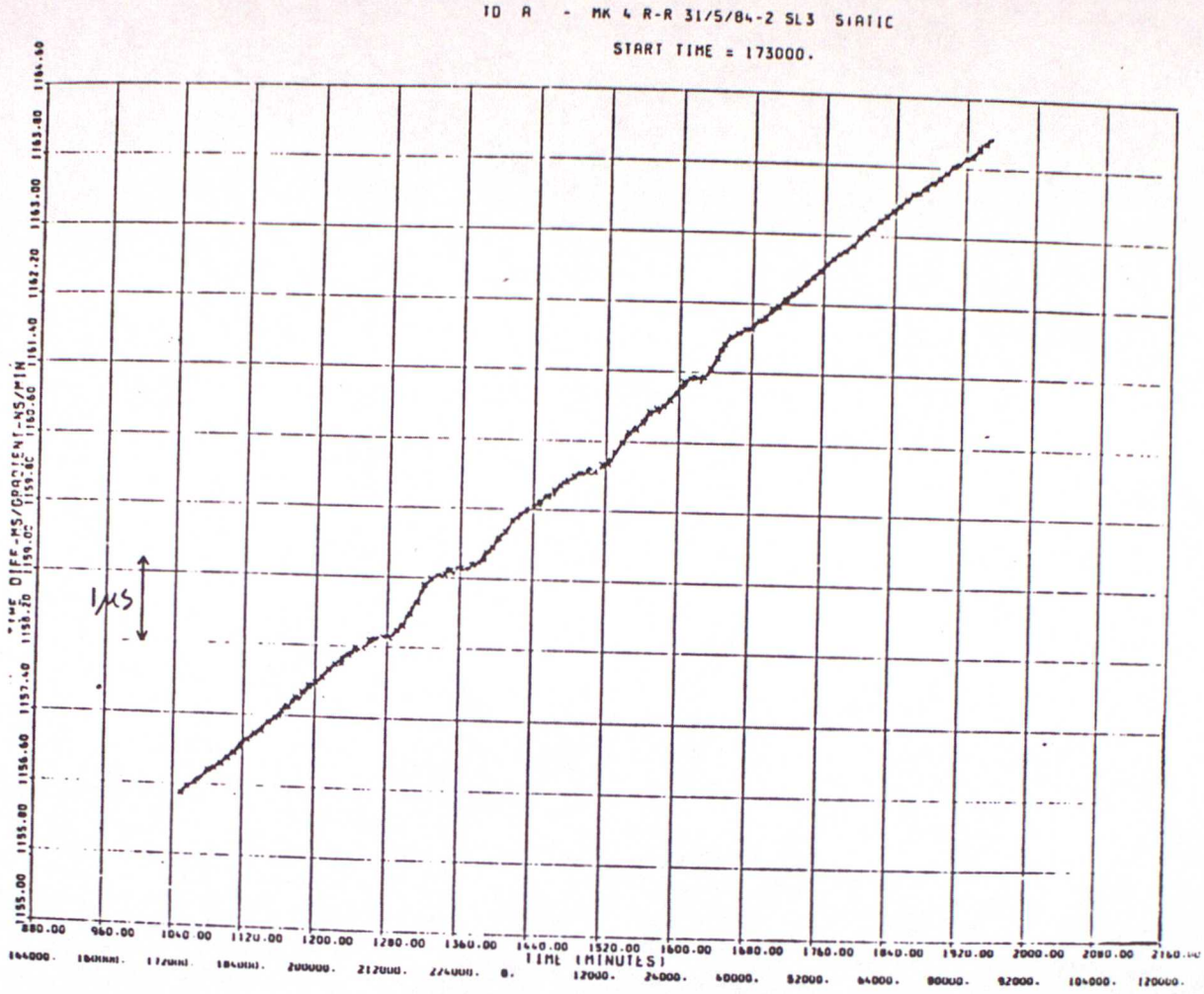

4(c) Sandur (range 1650km).

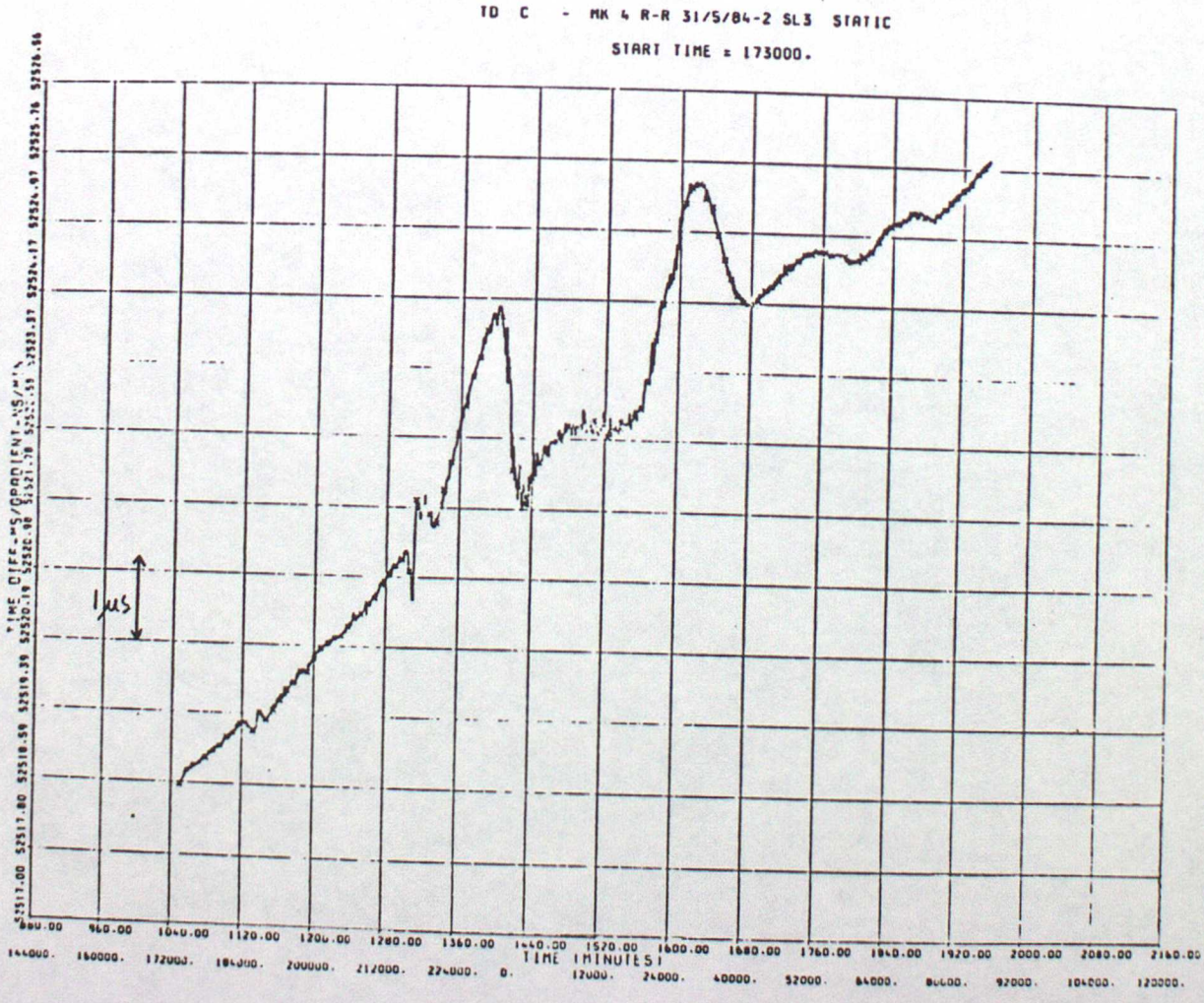

Fig.5 - Graph of standard deviation of time of arrival gradient plotted against SNR for static monitoring of the SL3 Loran-C chain using the Beukers LOCATE system.

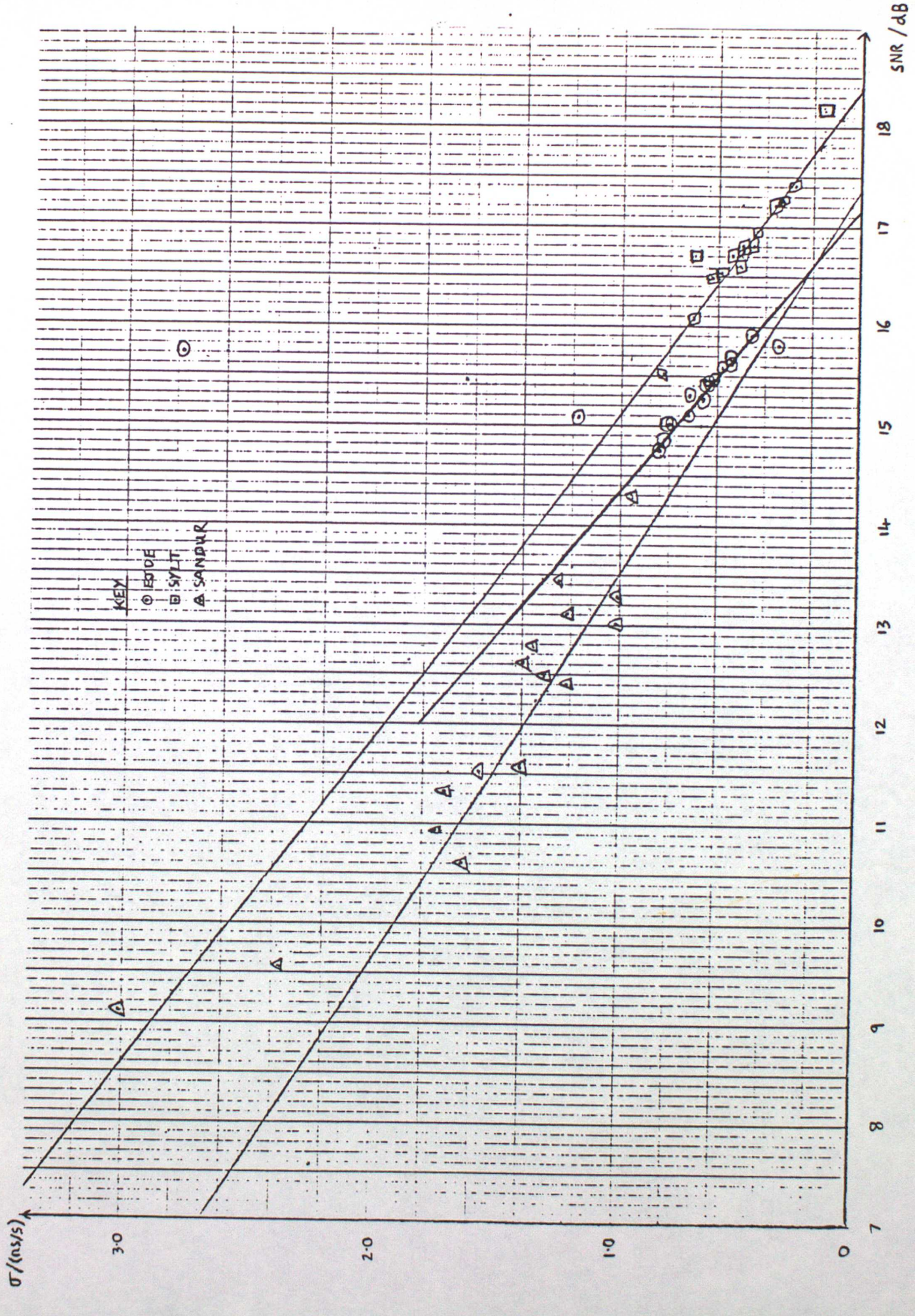

Fig.6 - Graph of standard deviation of time of arrival gradient plotted against SNR for static monitoring of the SL3 and French Loran-C chains using the new dropsonde system.

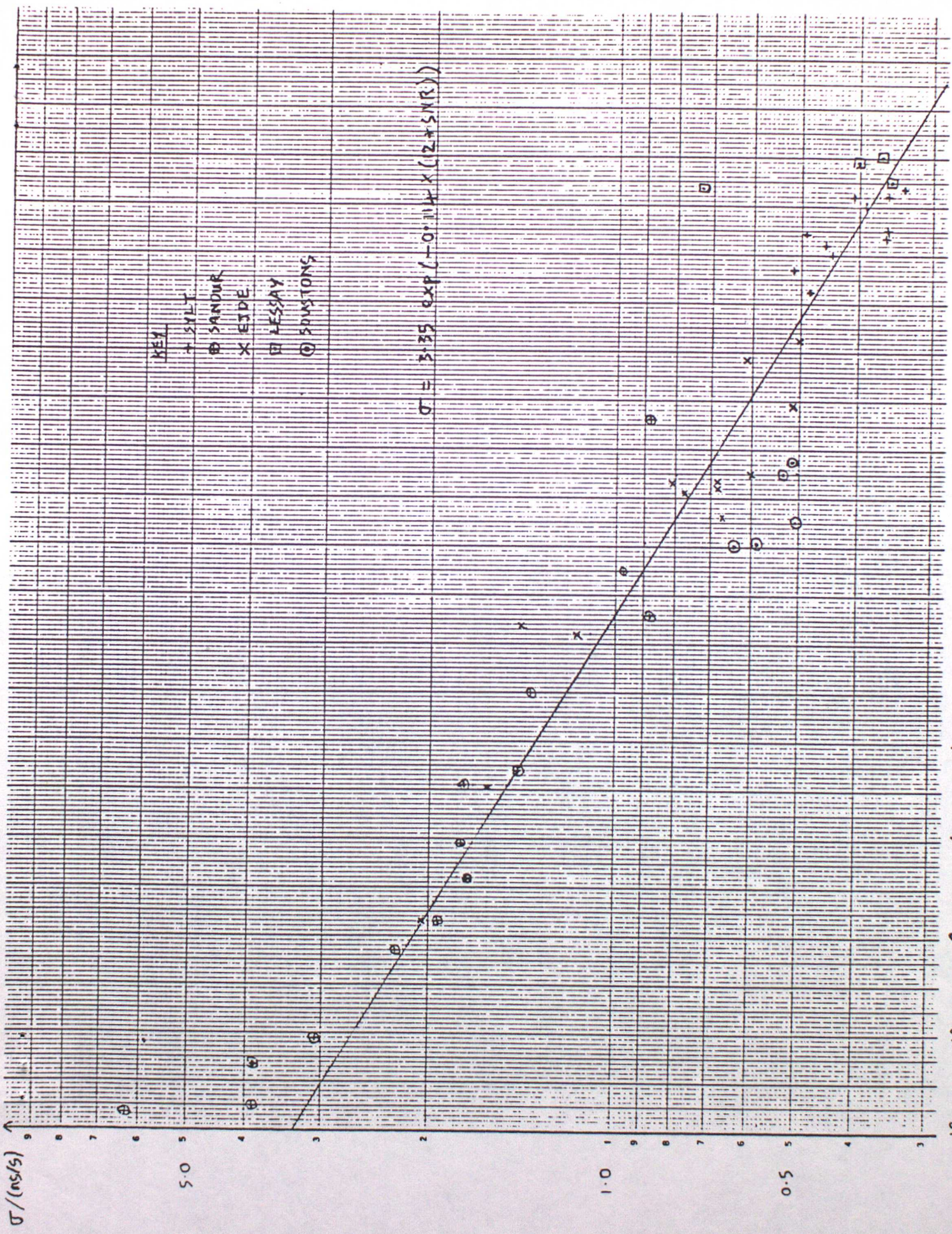

Fig.7 - One-minute winds and vector differences derived from radar and Loran for Flight 1.

(a)

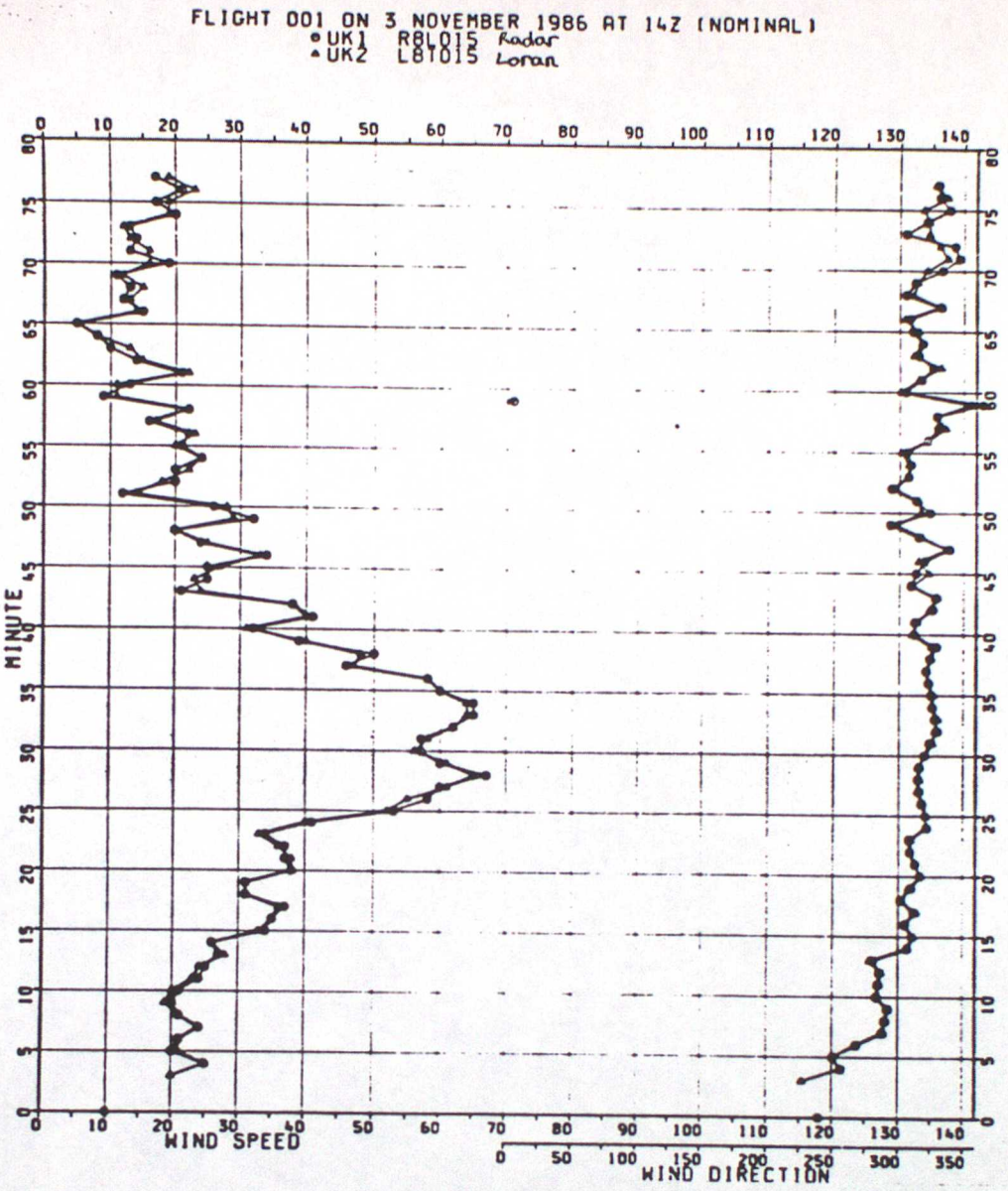

(b)

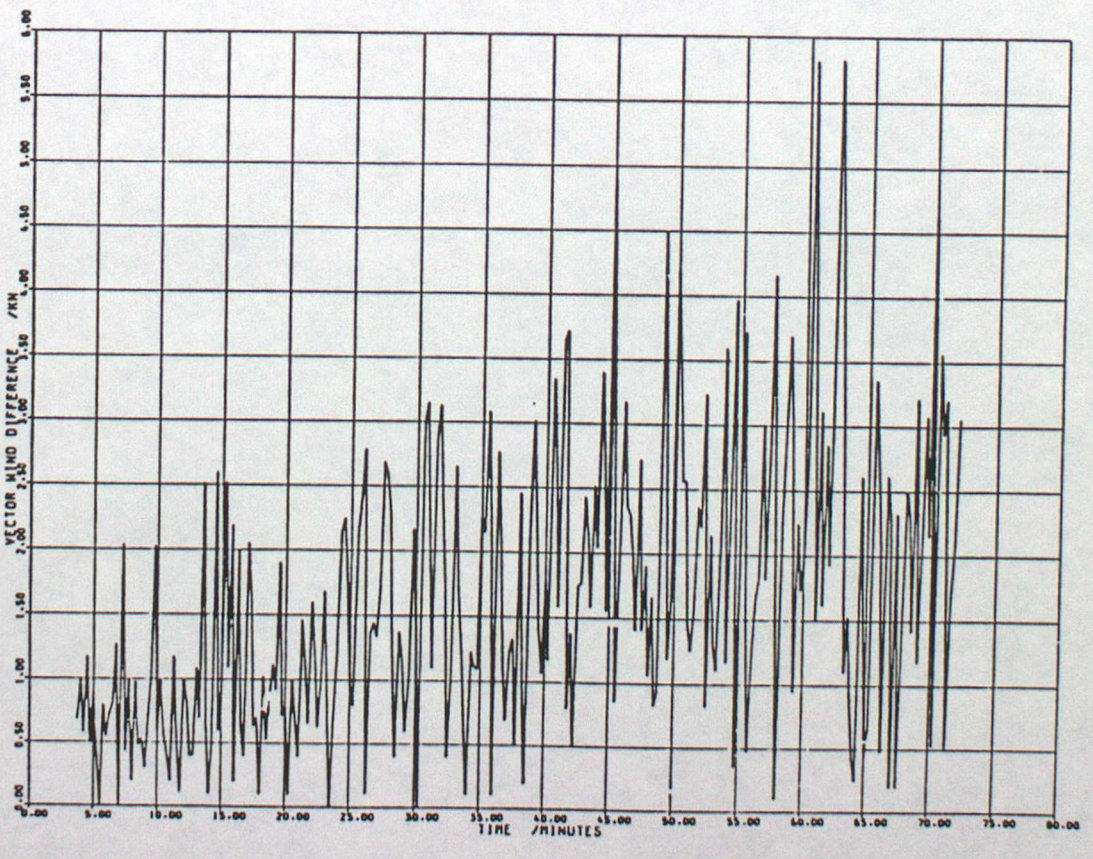

Fig.8 – One-minute winds and vector differences derived from radar and Loran for Flight 2.

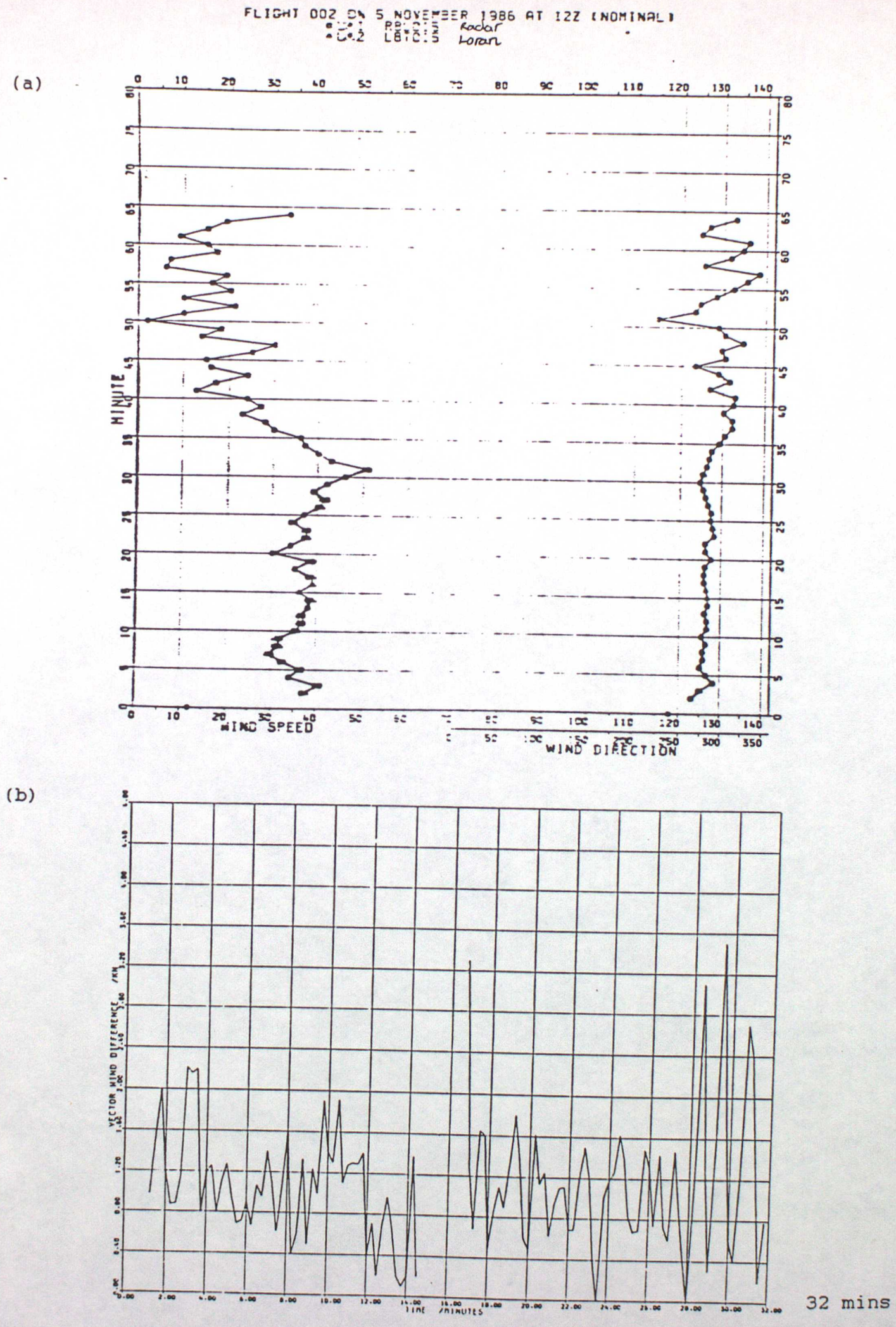

Fig.9 - One-minute winds and vector differences derived from radar and Loran for Flight 3.

(a)

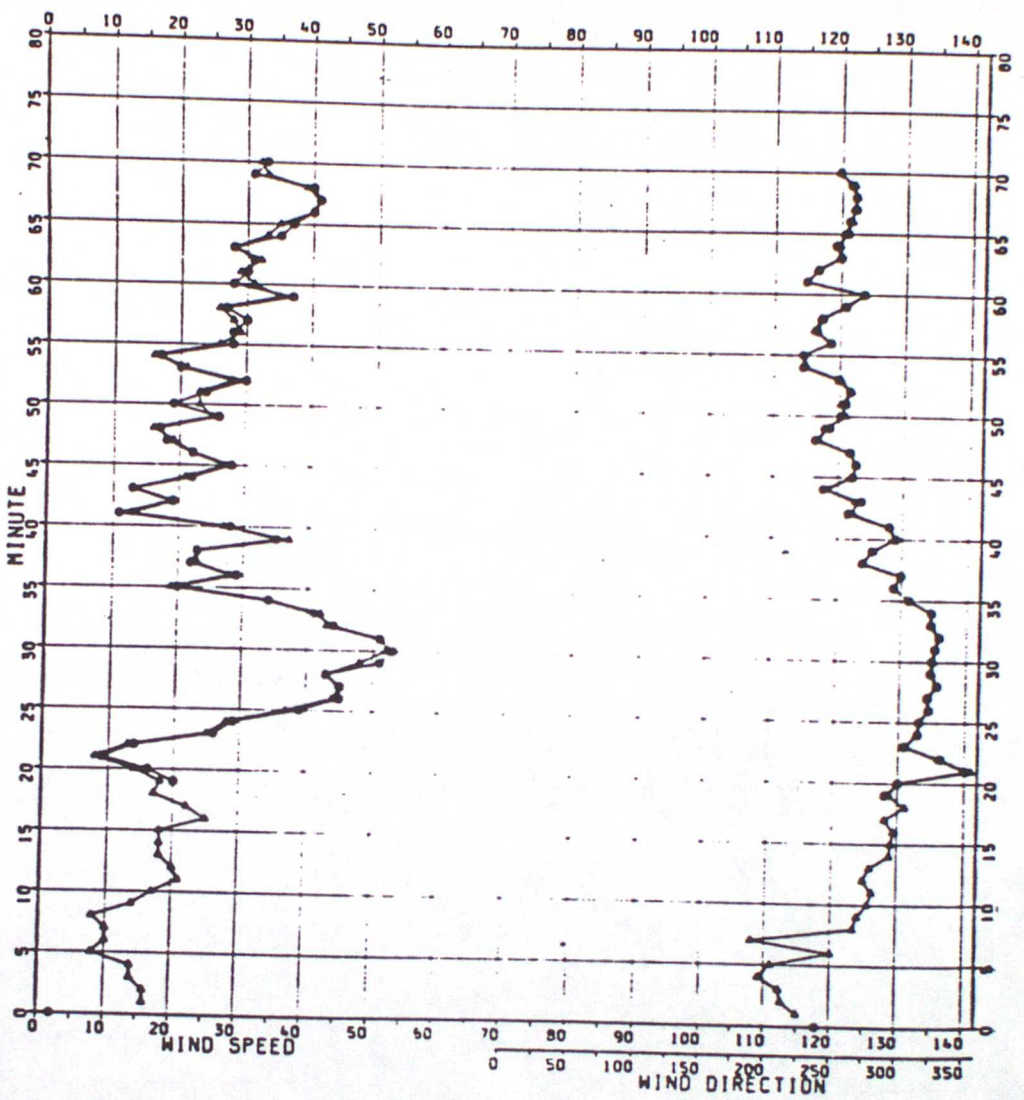

(b)

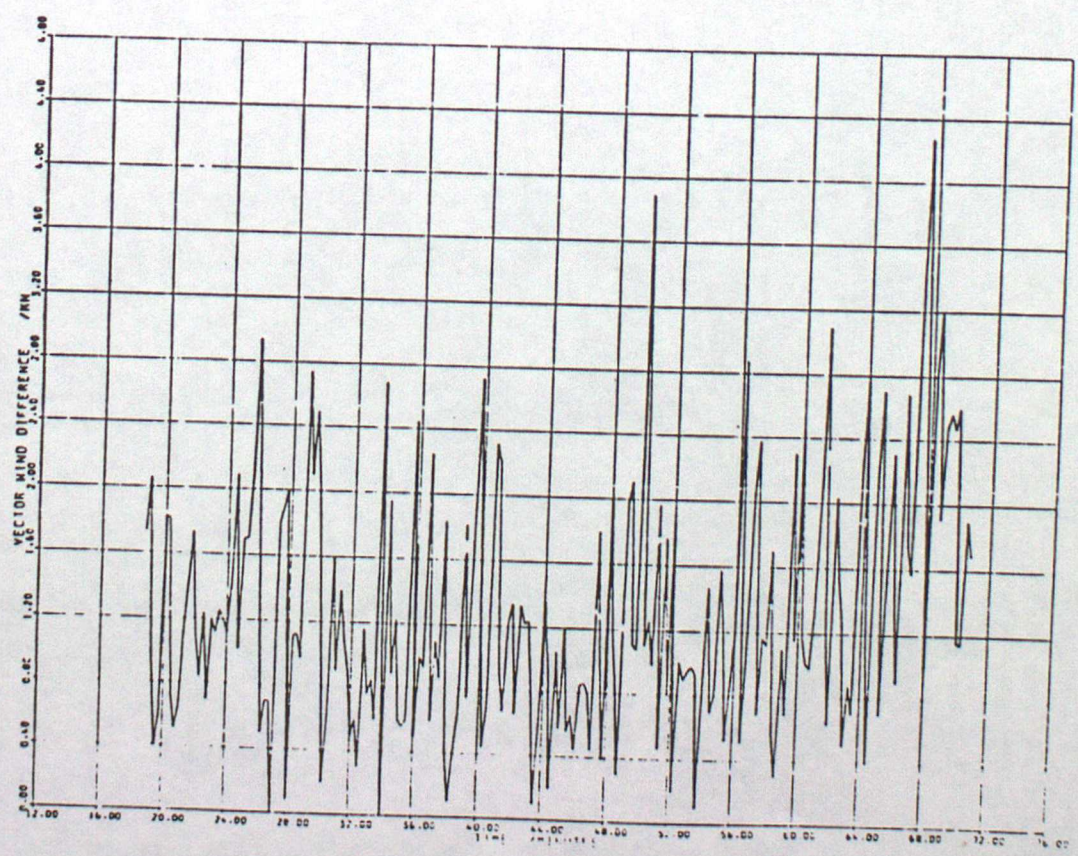

Fig.10 - One-minute winds and vector differences derived from radar and Loran for Flight 4.

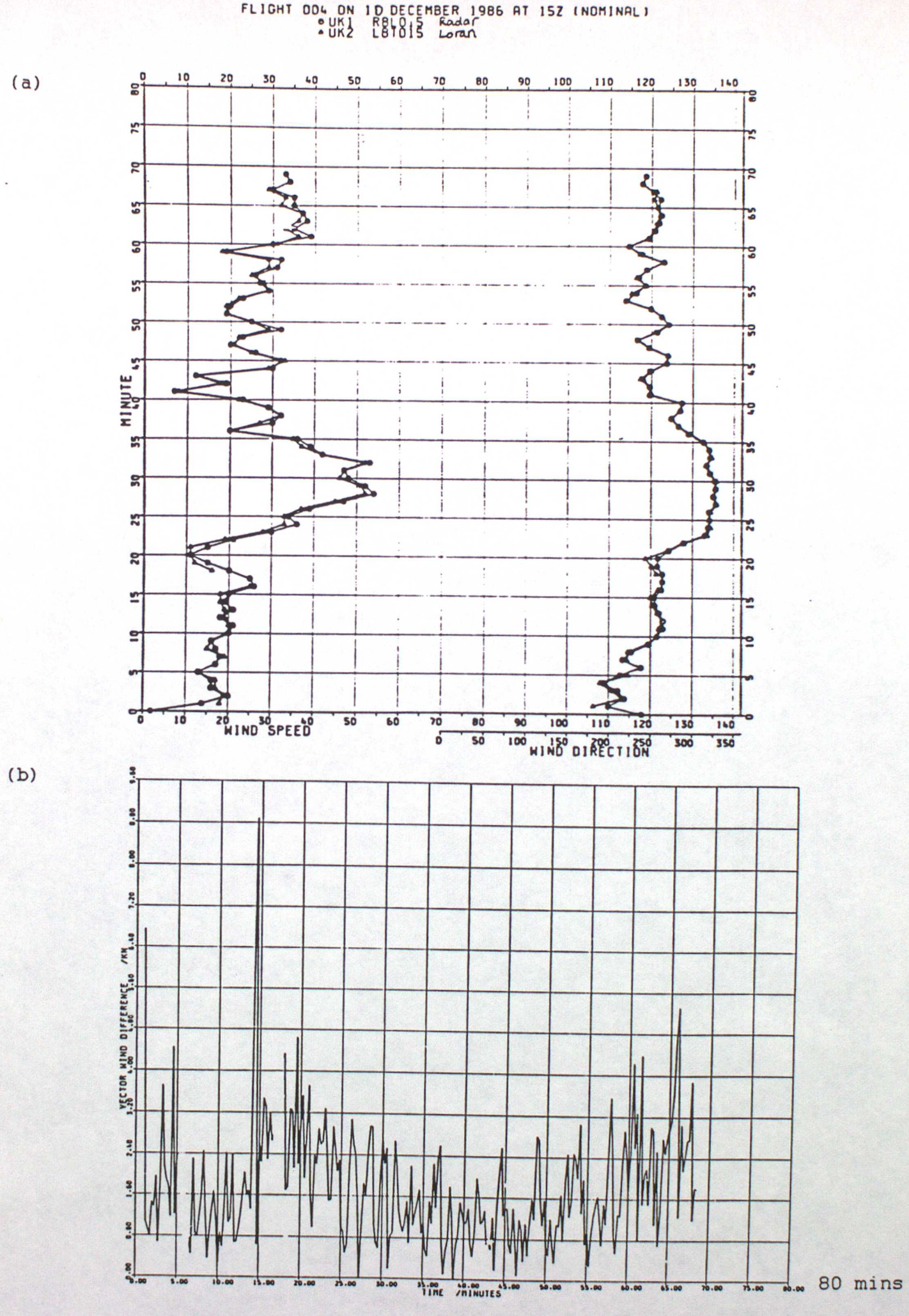

Fig.11 - One-minute winds and vector differences derived from radar and Loran for Flight 5.

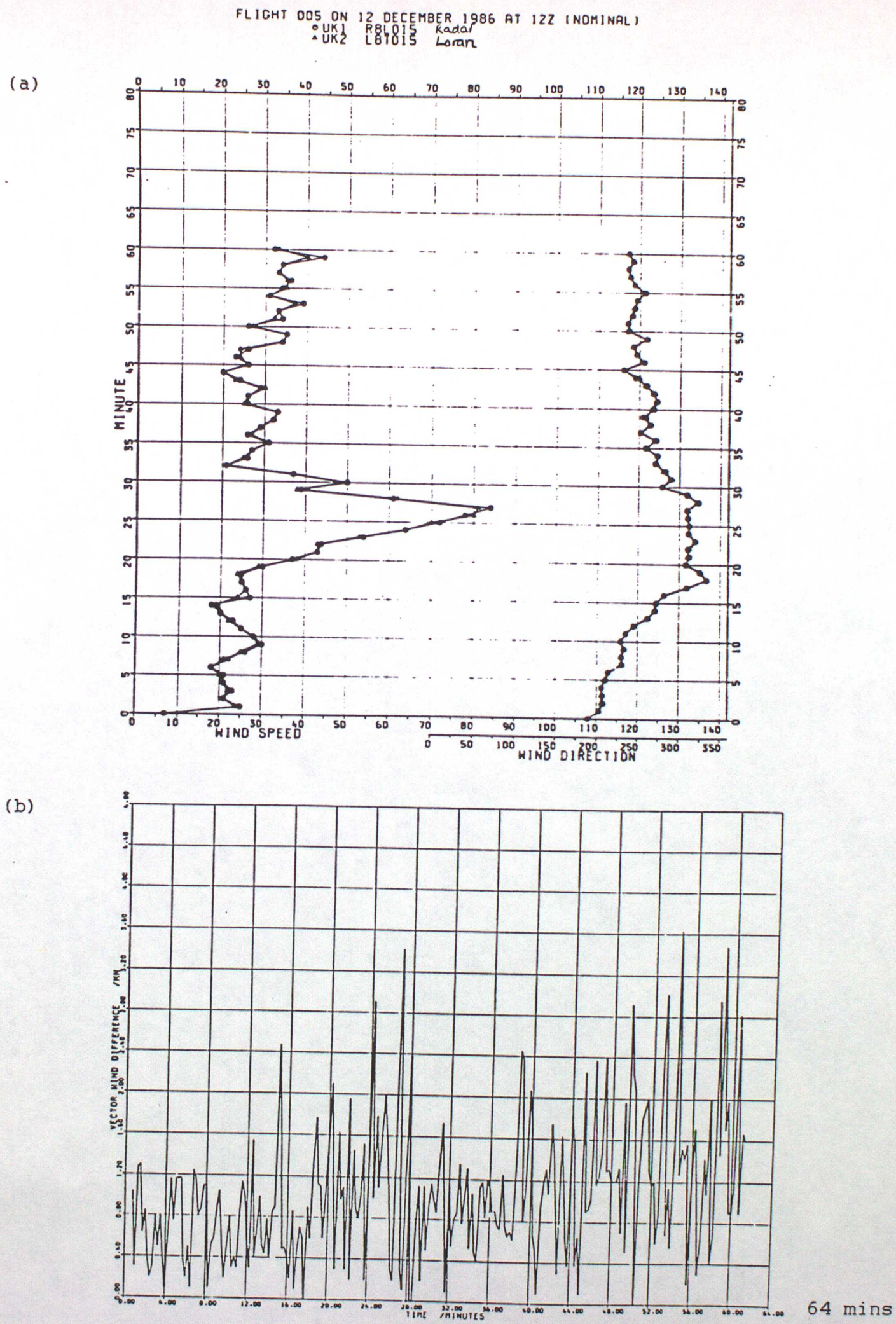

Fig.12 - One-minute winds and vector differences derived from radar and Loran for Flight 6.

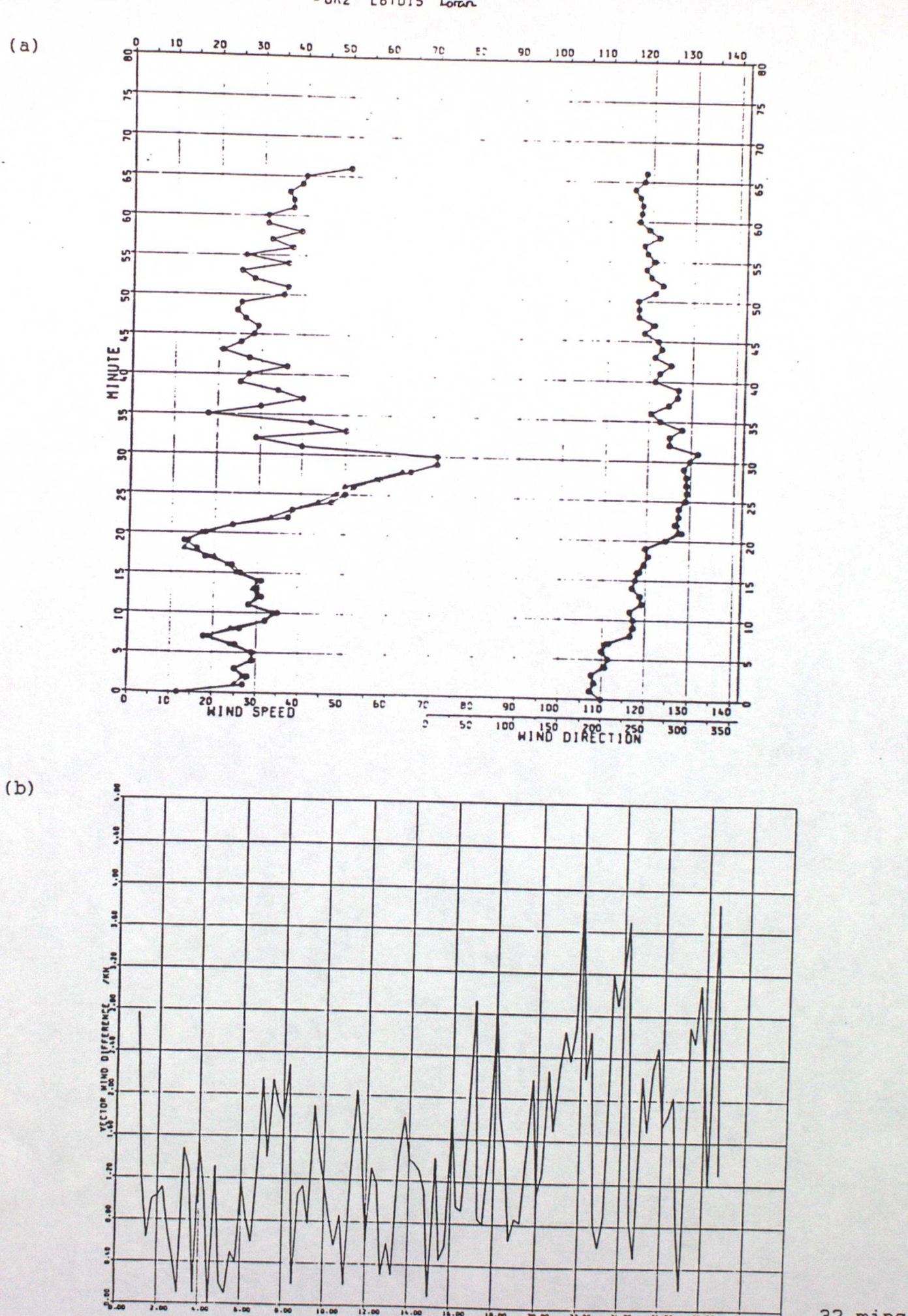

Fig.13 - Difference between radar and Loran component velocities for Flight 5.

(a) - U-component difference (radar - Loran).

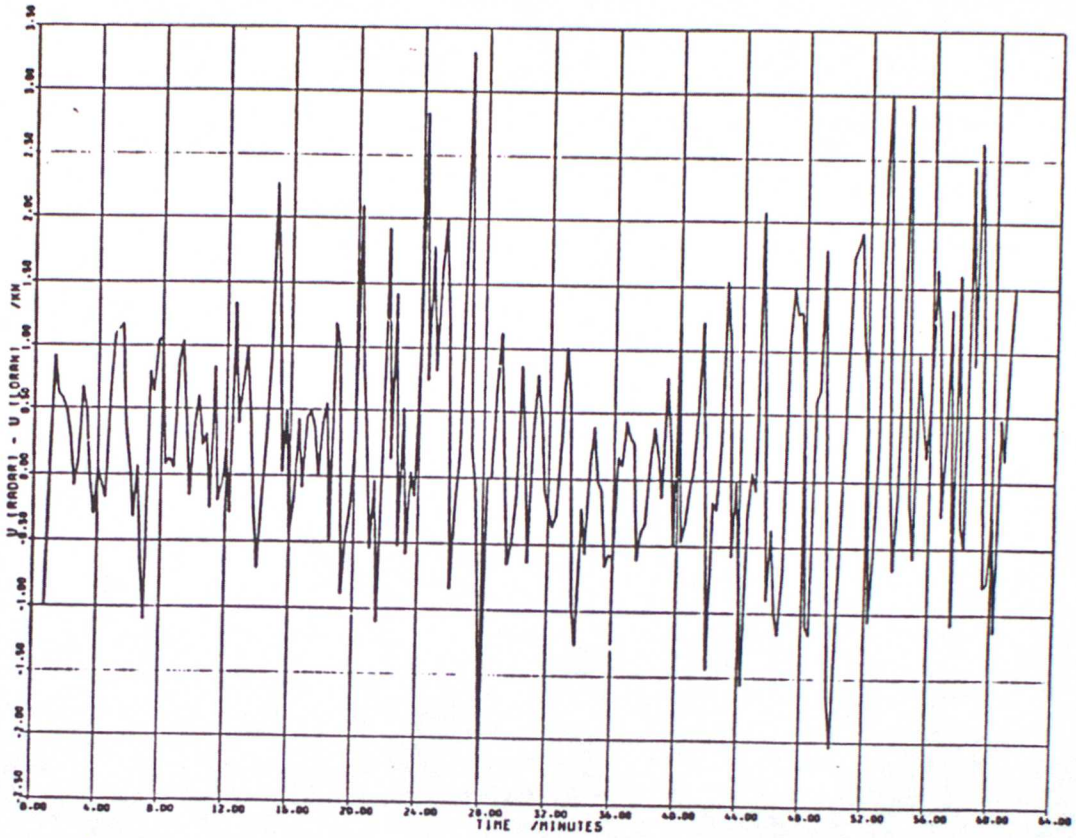

(b) - V-component difference (radar - Loran).

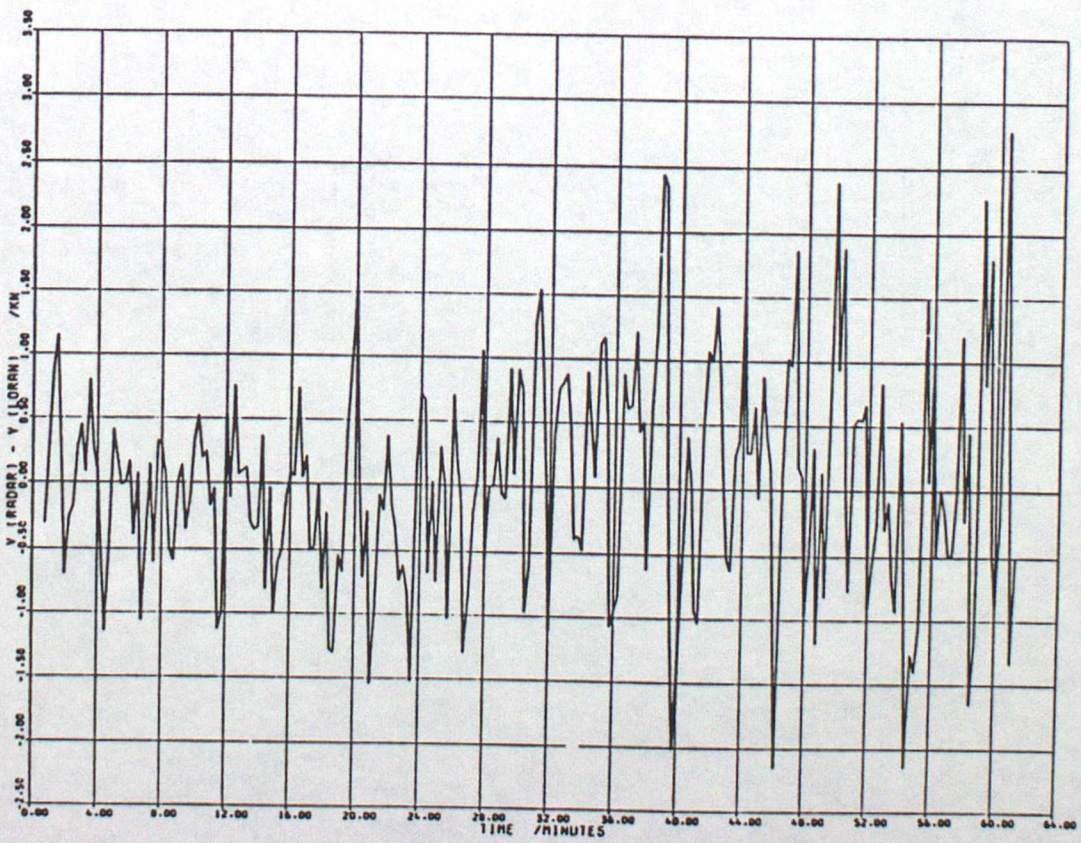

Fig.14 - Graphs of SNR for each transmitter plotted against time for Flight 4.

14(a) - Sylt.

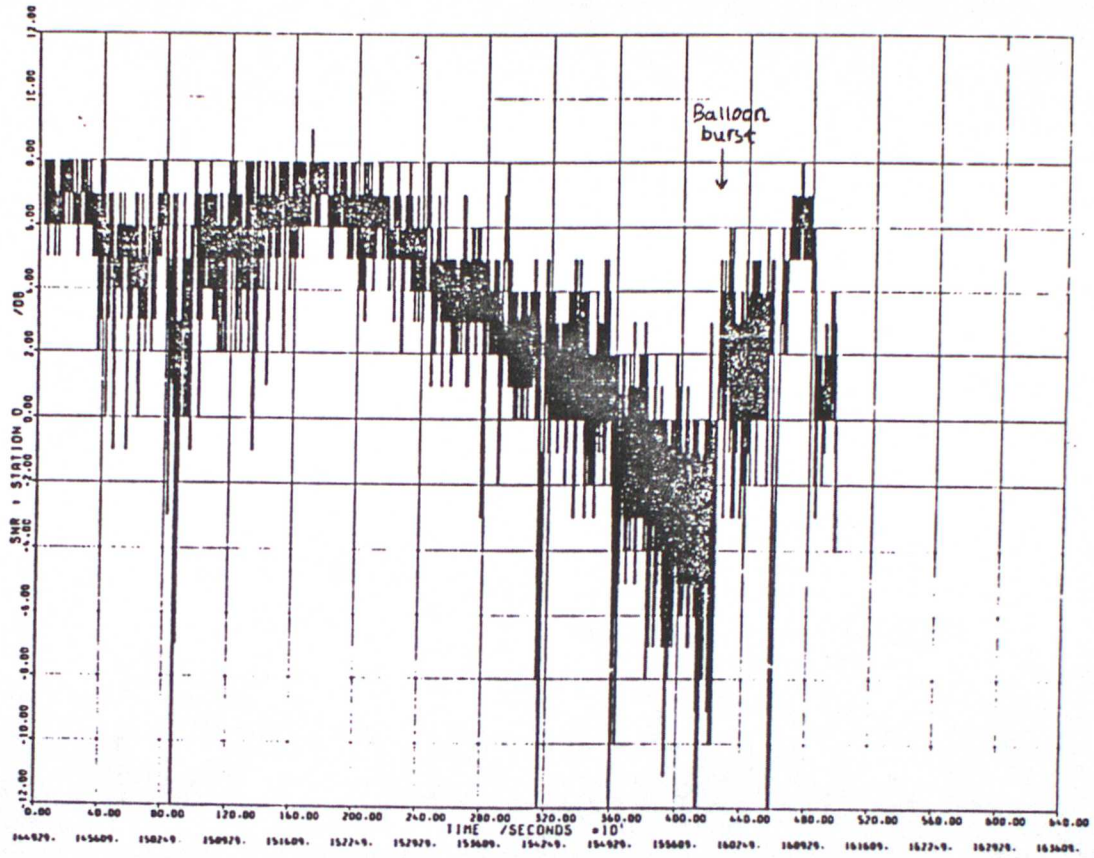

14(b) - Sandur. (Not used in calculations.)

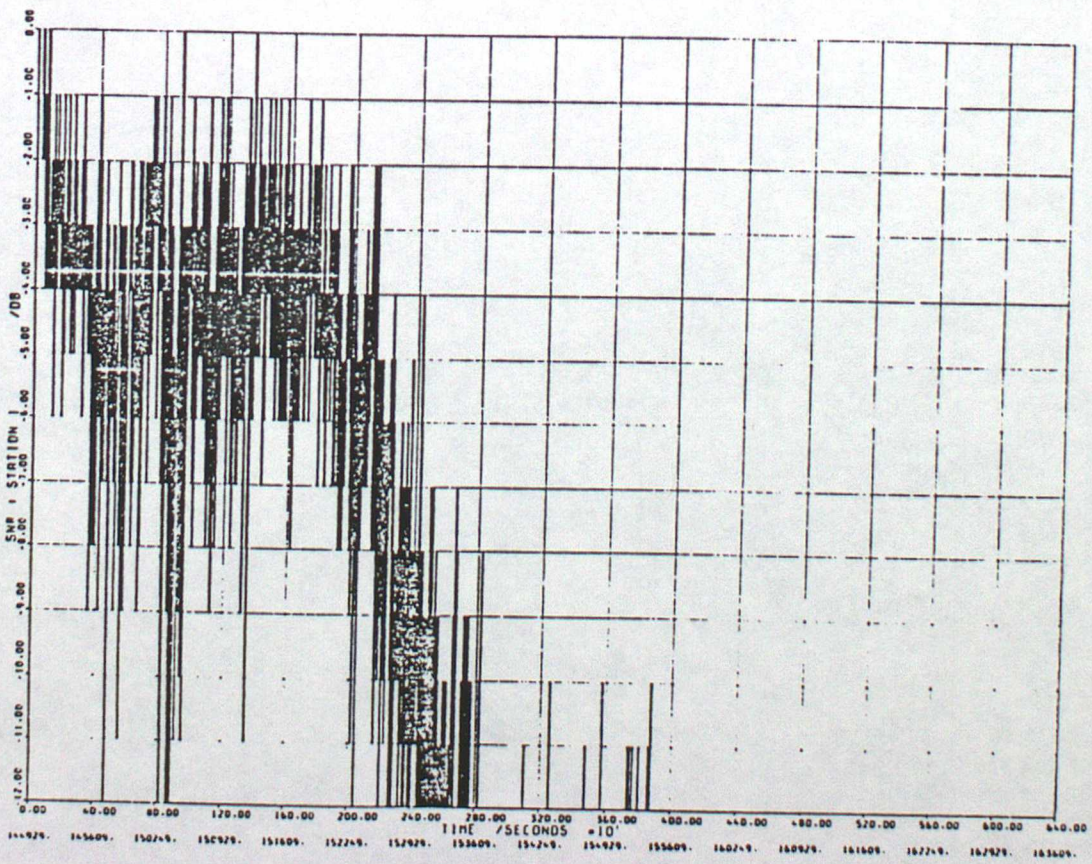

14(c) - Ejde. (Poor signal quality at the beginning and end of the flight.)

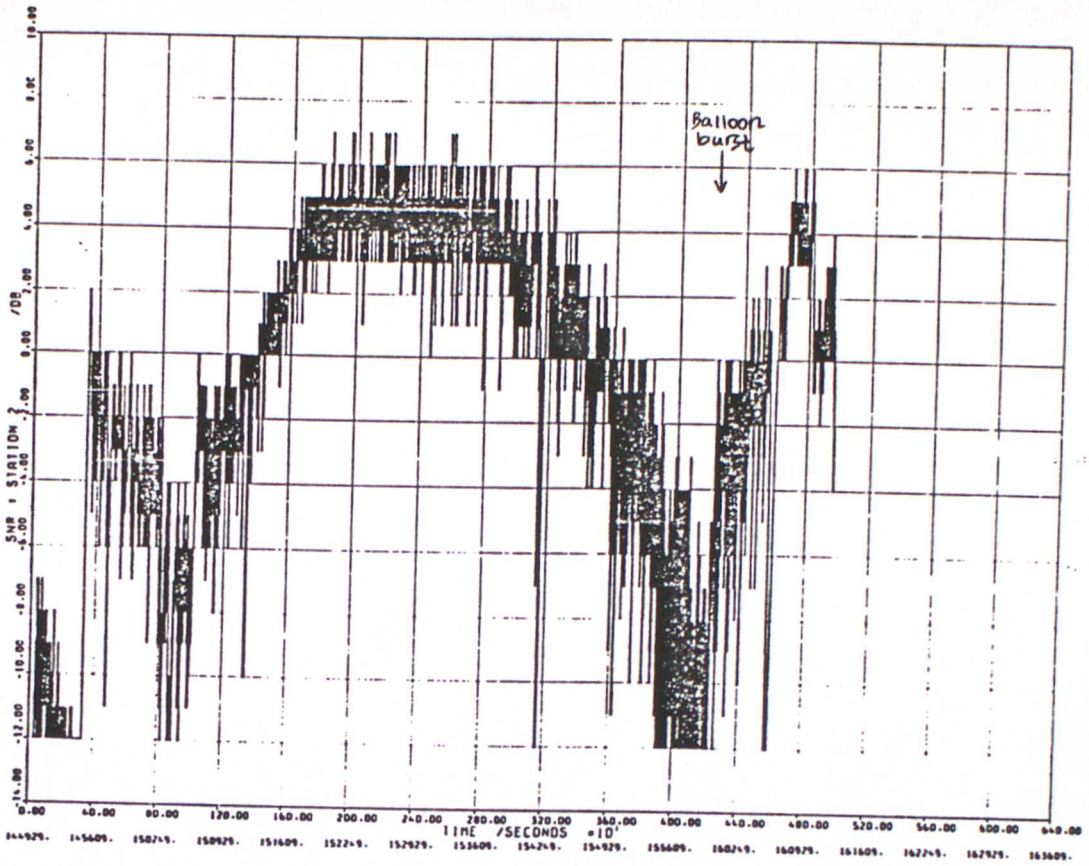

14(d) - Lessay.

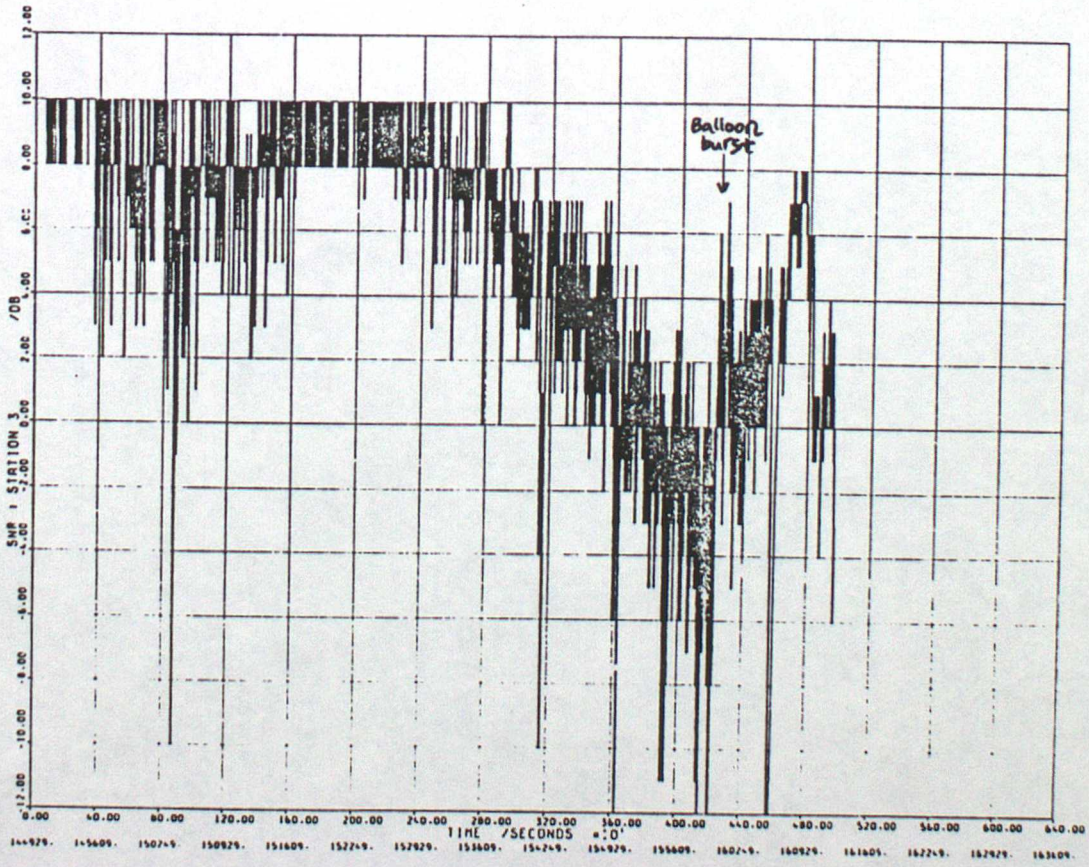

14(e) - Soustons.

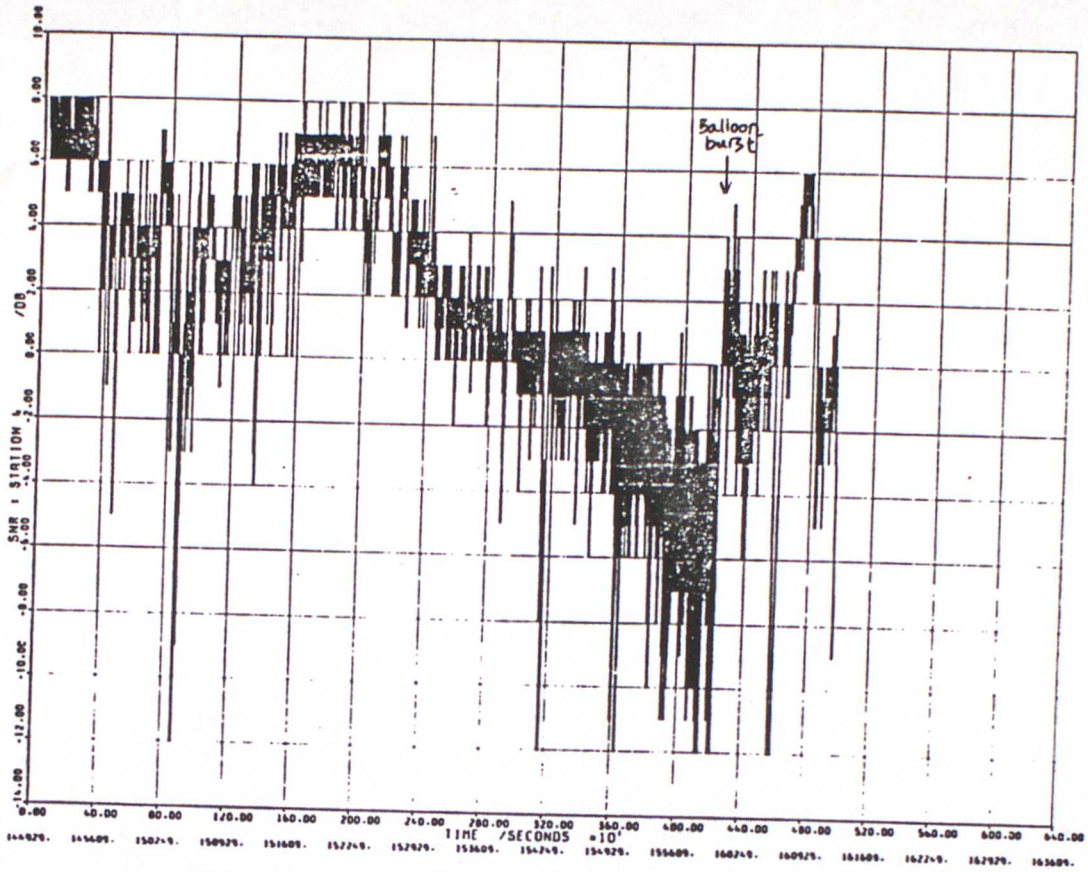

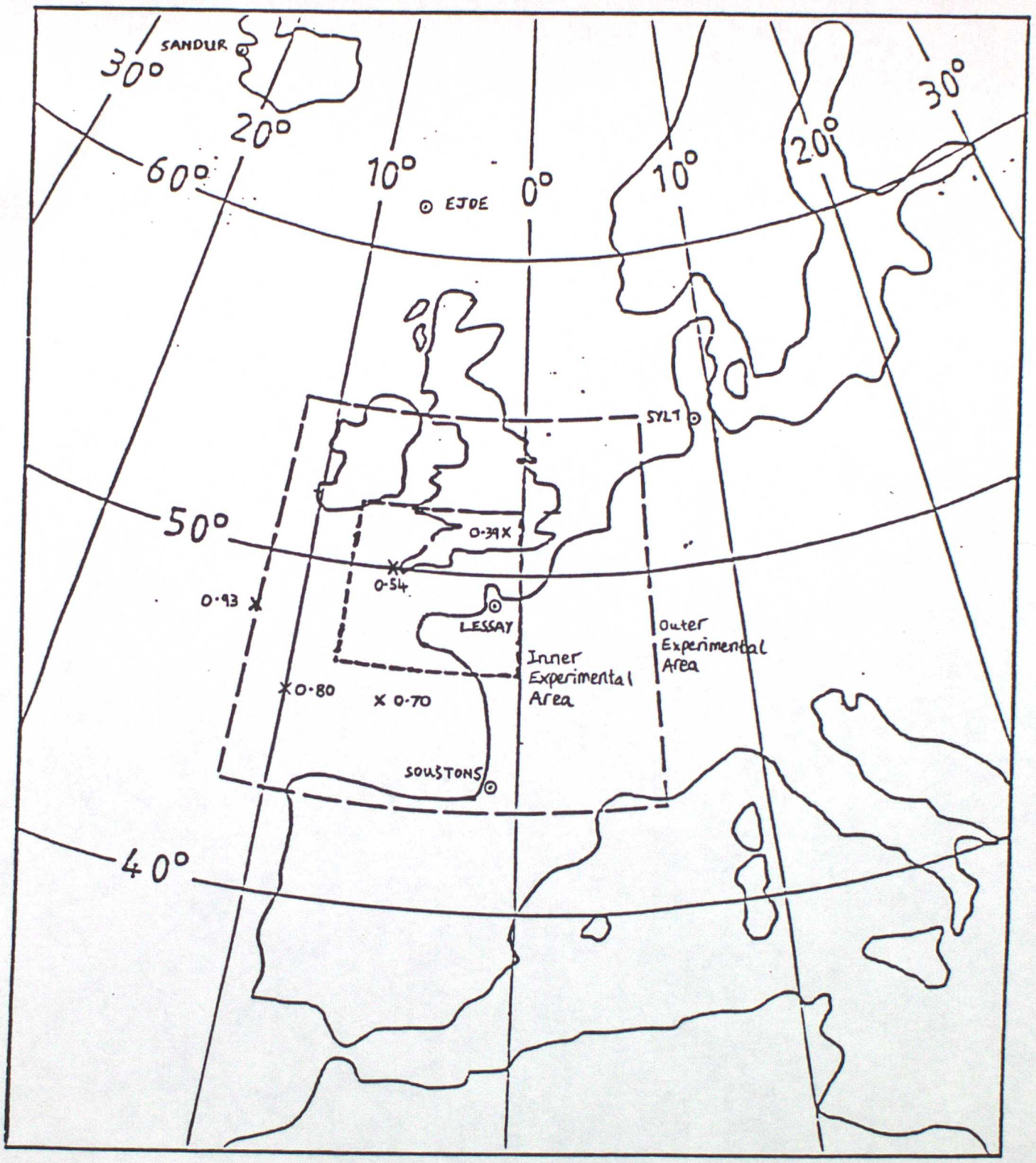

Fig.15 - Estimated RMS wind measurement accuracy (dU) in knots for selected points in the experimental area of the Mesoscale Frontal Dynamics Project. Approximate positions of Loran transmitters are also shown.

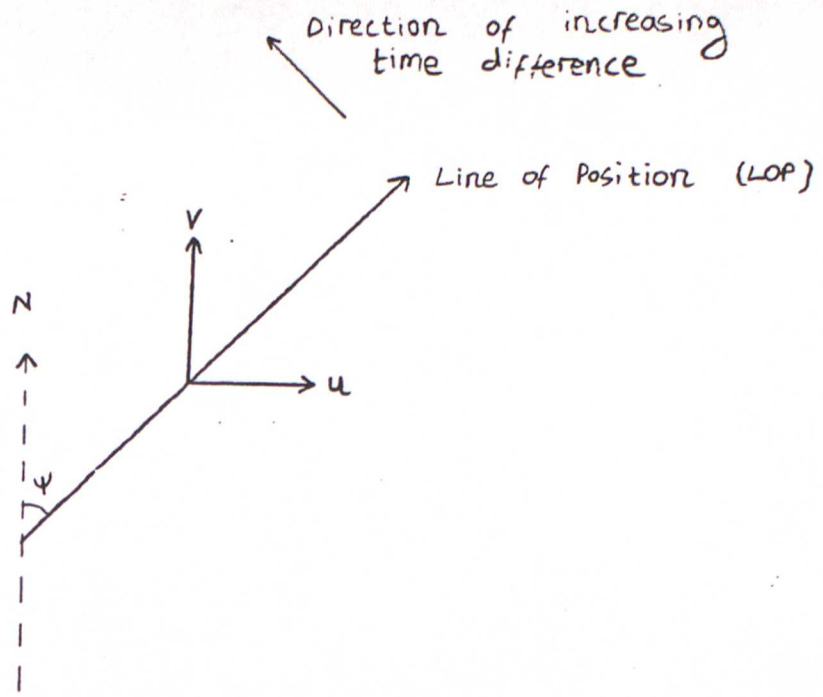

Fig.16 - LOP geometry.